

4

MARTIN MARIETTA ENERGY SYSTEMS LIBRARIES



3 4456 0364241 3

CENTRAL RESEARCH LIBRARY  
DOCUMENT COLLECTION

ORNL-3069  
UC-34 - Physics  
TID-4500 (16th ed.)

MEASUREMENTS AT BEAM HOLE HB-2 OF THE  
OAK RIDGE RESEARCH REACTOR FOR SOUTH  
FACILITY MOVABLE SHIELD DESIGN STUDY

F. J. Muckenthaler  
T. V. Blosser  
J. M. Miller  
L. Jung

CENTRAL RESEARCH LIBRARY  
DOCUMENT COLLECTION  
**LIBRARY LOAN COPY**  
**DO NOT TRANSFER TO ANOTHER PERSON**  
If you wish someone else to see this  
document, send in name with document  
and the library will arrange a loan.



**OAK RIDGE NATIONAL LABORATORY**  
operated by  
**UNION CARBIDE CORPORATION**  
for the  
**U.S. ATOMIC ENERGY COMMISSION**

Printed in USA. Price \$1.00 Available from the

Office of Technical Services  
Department of Commerce  
Washington 25, D. C.

#### LEGAL NOTICE

This report was prepared as an account of Government sponsored work. Neither the United States, nor the Commission, nor any person acting on behalf of the Commission:

- A. Makes any warranty or representation, expressed or implied, with respect to the accuracy, completeness, or usefulness of the information contained in this report, or that the use of any information, apparatus, method, or process disclosed in this report may not infringe privately owned rights; or
- B. Assumes any liabilities with respect to the use of, or for damages resulting from the use of any information, apparatus, method, or process disclosed in this report.

As used in the above, "person acting on behalf of the Commission" includes any employee or contractor of the Commission, or employee of such contractor, to the extent that such employee or contractor of the Commission, or employee of such contractor prepares, disseminates, or provides access to, any information pursuant to his employment or contract with the Commission, or his employment with such contractor..

Contract No. W-7405-eng-26

Neutron Physics Division

MEASUREMENTS AT BEAM HOLE HB-2 OF THE OAK RIDGE RESEARCH REACTOR  
FOR SOUTH FACILITY MOVABLE SHIELD DESIGN STUDY

F. J. Muckenthaler      J. M. Miller  
T. V. Blosser            L. Jung

DATE ISSUED

AUG 31 1961

OAK RIDGE NATIONAL LABORATORY  
Oak Ridge, Tennessee  
operated by  
UNION CARBIDE CORPORATION  
for the  
U. S. ATOMIC ENERGY COMMISSION



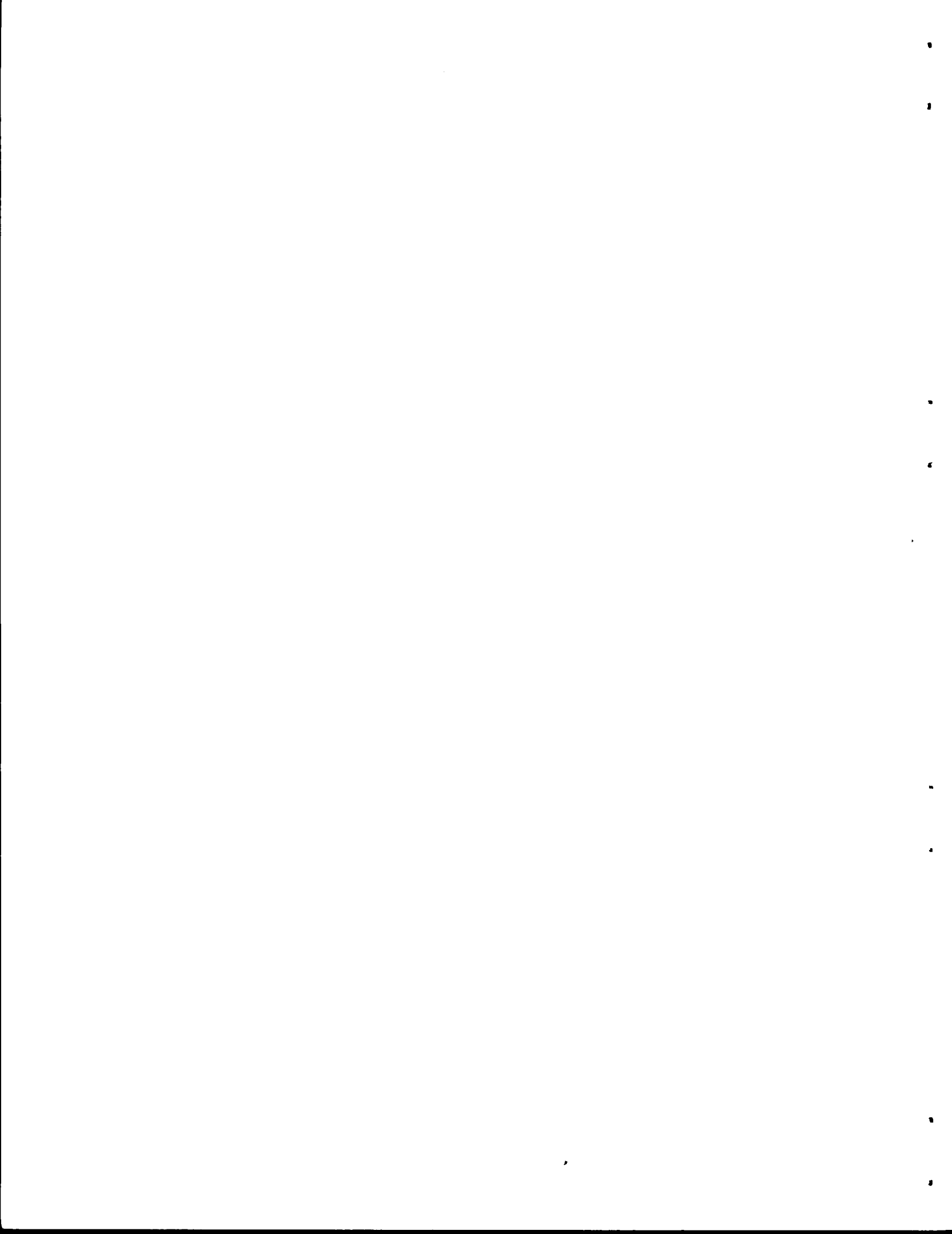
3 4456 0364241 3

TABLE OF CONTENTS

	<u>Page No.</u>
Abstract . . . . .	iii
Introduction . . . . .	1
Description of Experiment . . . . .	2
Experimental Procedure . . . . .	7
Experimental Results . . . . .	11
Neutron Spectra . . . . .	11
Fast-Neutron Dose Rates . . . . .	11
Gamma-Ray Dose Rates . . . . .	26

## ABSTRACT

A series of measurements have been completed at Beam Hole HB-2 of the ORR, for use in designing a movable personnel and instrument shield for the ORR South Facility. They include thermal and fast-neutron spectra, both unattenuated and behind selected shield configurations, and fast-neutron and gamma dose rates behind about 38 configurations. Materials used for the shield mockups included lead, iron, borated polyethylene, polyethylene and concrete. An attempt was also made to measure the intensity of the scattered radiation from these configurations. Despite experimental complications, some general conclusions have been drawn from the latter experiments.



## INTRODUCTION

A test loop, to be used for evaluation of gas-cooled reactor fuel elements, has been proposed for installation at the South Facility of the Oak Ridge Research Reactor. The installation requires a movable shield, both for the protection of personnel and electronic equipment during loop operation and for the protection of personnel working within the stationary shield during loop shutdown. The requirements for this shield are rather stringent, including a specified volume, light weight, ready mobility, and a minimum of scattered radiation. Since little data is available concerning the leakage characteristics of this relatively new reactor, a series of experiments has been performed to obtain the required design information. It would have been desirable, of course, to have performed these experiments at the South Facility itself. However, this would have required an external shield which was not readily available. Time was important, and the cost of fabrication of a shield was prohibitive for such a short-term experiment. Beam hole HB-2, which has a permanent external shield, was accessible at the time, and since the spectra from this smaller-diameter hole should closely approximate that from the 10-in.-dia beam hole, HS-1, at the South Facility, the data was obtained at HB-2.

The measurements performed include neutron spectra, both unattenuated and after passing through selected shield configurations, and fast-neutron and gamma-ray dose rates behind various combinations of iron, lead, barytes concrete, polyethylene, and borated polyethylene slabs. An attempt was also made to observe the relationship of the scattered

component to the transmitted component of both neutron and gamma radiation with several of the materials noted above. From the latter measurements only general conclusions can be drawn, because of complicating experimental effects.

### DESCRIPTION OF EXPERIMENT

#### Facility

The existing personnel shield surrounding Beam Hole HB-2 consists mainly of barytes concrete, in three sections, with iron chips added to the top section. The bottom section contains no voids and is stationary. The center section (see Fig. 1) is roughly horseshoe-shaped, resulting in an air gap about 18 in. wide, 35 in. long, and 36 in. high, centered on the emergent beam. The top section of the shield contains two vertical ducts, each approximately six inches in diameter and positioned near opposite ends of the air gap of the center section. The centerlines of the ducts intersect the centerline of the emergent beam. A 27-in.-long steel-lined concrete coffin, shown in Fig. 2, was centered on the emergent beam in the air gap of the center section, and contained the shielding samples. The samples were uniformly 12 in. square, with edges machined to a close fit to the coffin to reduce edge streaming. In the case of the barytes concrete samples, a 3/16-in.-thick iron band surrounding the sample edges provided the close fit and also minimized damage during handling. Since the coffin was open-ended, measurements could be made directly behind the shielding configurations. Entry of the beam into the coffin was controlled by a

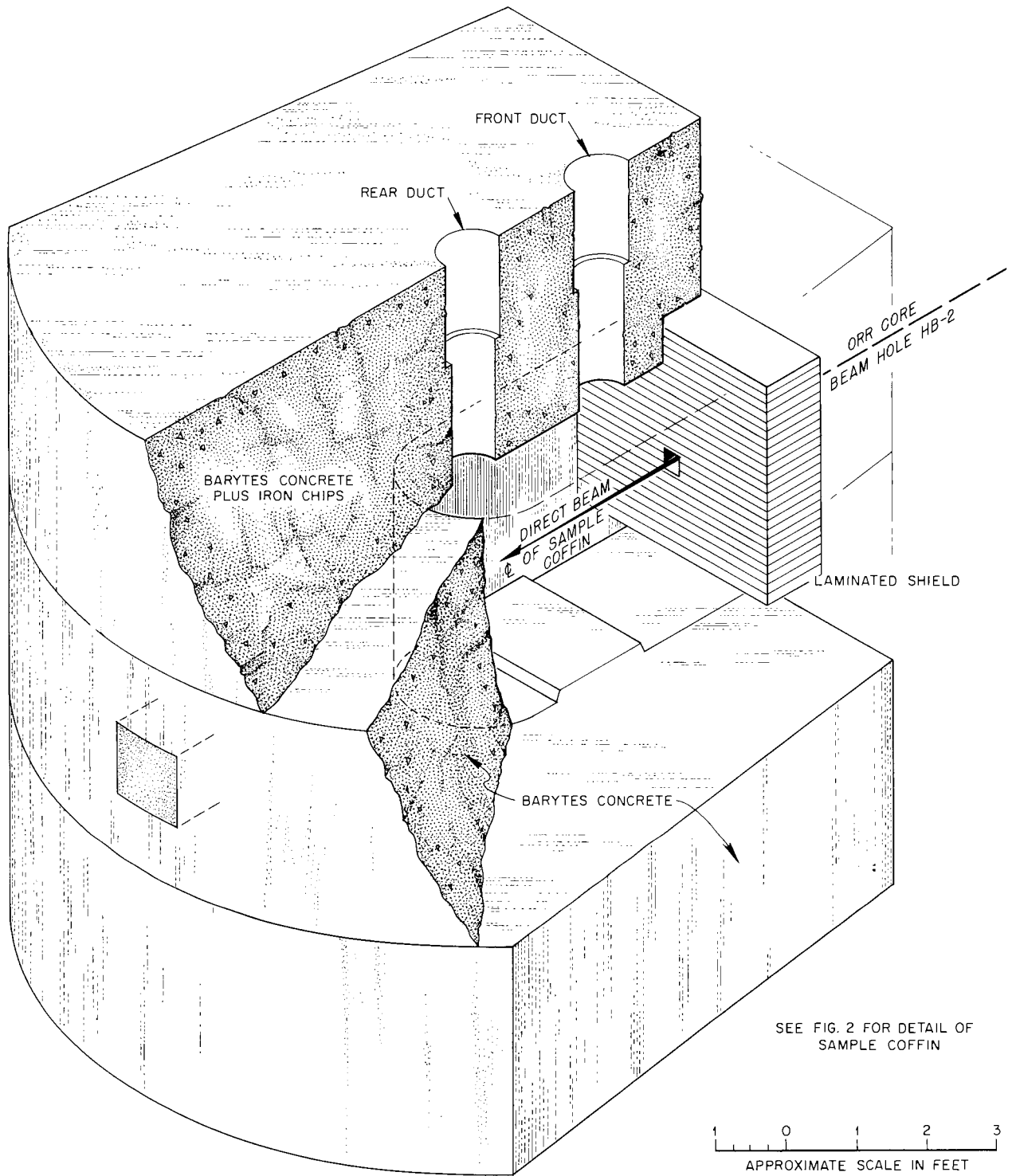


Fig. 1. Permanent Personnel Shield, Beam Hole HB-2, ORR.

UNCLASSIFIED  
ORNL-LR-DWG 54930

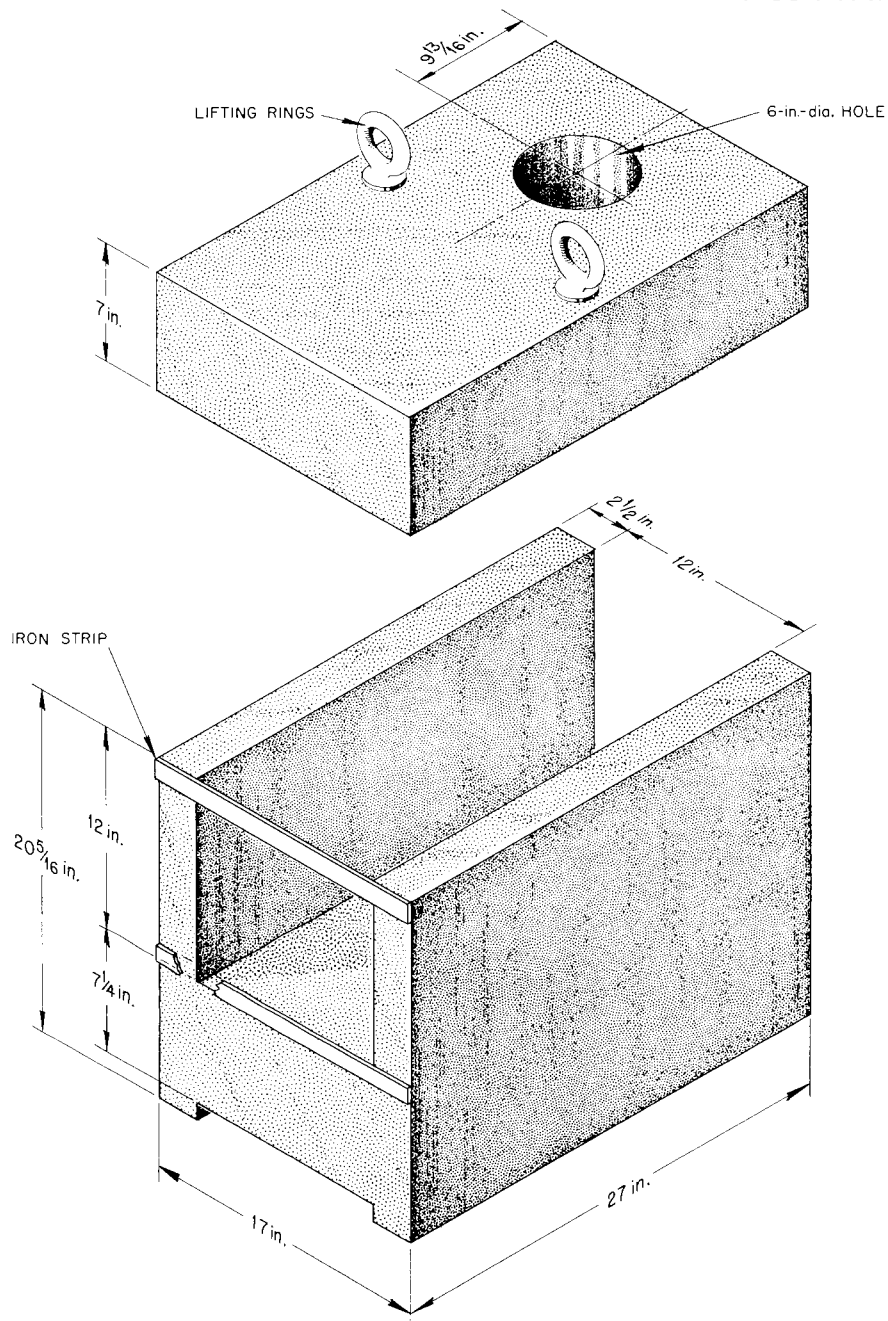


Fig. 2. Concrete Coffin Used for Positioning Shield Samples.

rotatable, 24-in.-thick, laminated iron and masonite plug. The plug contained both a 3-in.-square and a 1/2-in.-square opening, with most measurements being made using the 3-in.-square hole.

Changes in the shield configurations were made by filling the inner tank in the beam hole with water and removing the top section of the personnel shield with the overhead crane. The top of the sample coffin could then be removed and configurations changed. The top section of the personnel shield was marked to insure accurate replacement.

The two 6-in.-dia ducts in the top shield were utilized for instrument access, as well as for the series of measurements of the scattered component of the neutron and gamma radiation noted above. For this series 6-in.-dia disks of lead, polyethylene, borated polyethylene, and concrete, closely fitting the duct, were used in attenuation measurements. The concrete disks were surrounded by a 1/16-in.-thick iron band for protection.

For convenience in discussion, these disks, when placed to attenuate the radiation in the ducts, are called "absorbers;" materials placed in the direct beam are called "shield samples" or "shield configurations."

An analysis of the barytes concrete used in these experiments is contained in Table 1. The borated polyethylene contained 0.91 wt % boron.

Table 1. Chemical Analysis of Barytes Concrete  
Samples from HB-2 Experiments

Element	Weight Per Cent*
O	34.52
Ba	28.40
Ca	13.05
Fe	10.53
S	6.63
Si	2.45
Mg	2.10
Al	1.37
H	0.78
K	0.14
Na	0.03

\* Analysis was made as oxides and sulfates. Values of elements were obtained by application of appropriate gravimetric factors and normalized to 100%.

EXPERIMENTAL PROCEDURE

Gold foils were used to map the flux inside the personnel shield so that the center line of the emergent beam could be located. The foils were placed 1 cm apart on two aluminum strips which were at right angles to each other and perpendicular to the beam. The strips were fastened to a movable holder at the end of a lucite plug fitting into the vertical duct at the rear of the cavity in the personnel shield. From the induced activity in the foils the center of the beam was located, and subsequent foil exposures were positioned accordingly.

Thermal-neutron flux measurements, using bare and cadmium-covered gold foils, and fast-neutron spectral measurements, with both fission foils and sulfur pellets, were made both in the unattenuated beam and behind several shield configurations. The fission foils, Pu<sup>239</sup>, Np<sup>237</sup>, and U<sup>238</sup>, were arranged in that order within a boron sphere, which eliminated thermal-neutron activation. The sulfur pellets were irradiated by themselves, since the irradiation period was much longer than that for the foils.

Immediately following irradiation, decay activity of foils was measured with a NaI(Tl) scintillation counter and the saturation activity determined. Necessary corrections were applied, and the neutron flux at thermal energy and above each threshold energy was determined. From these spectra the total neutron dose rate was calculated. This result was normalized to correspond to the dose that would have been measured with a Hurst-type dosimeter by application of a factor derived from a supplementary experiment comparing foils and dosimeter.

Gamma-ray dose rates were measured with a 50-cc ion chamber and A-C electrometer, behind each shield configuration and in a series of scattered-dose measurements in the front duct. The ion chamber preamp housing was surrounded by a 2-ft-long piece of lucite, which served both as a shield plug during measurements and as a positioner for the various experiments. For the scattered dose measurements the detectors were positioned in the duct so that the absorber thickness could be varied up to 6 in. without changing the detector position. Measurements behind the configurations were always made prior to the fast-neutron dose rate measurements, so that the gamma-ray field would be known for the fast-neutron detector calibration. The ion chamber was calibrated against a  $\text{Co}^{60}$  source of known intensity.

Fast-neutron dose rate measurements with a Hurst-type dosimeter were made behind shield configurations when the gamma-ray dose rate did not exceed 30 r/hr. Like the ion chamber, the dosimeter preamp housing was surrounded by a lucite plug fitting either duct. For calibration, the detector was first exposed to a  $\text{Co}^{60}$  field corresponding to that previously measured by the ion chamber behind the shield configuration, and the amplifier gain adjusted to give  $\sim 25$  cpm at a PHS of 6 v. The  $\text{Co}^{60}$  source was then replaced by a Po-Be neutron source of known strength, and the count rate observed. From the dose-to-count-rate ratio thus obtained, the dose rate corresponding to the count rate measured behind the configuration was calculated.

A complete list of configurations for which neutron spectra, gamma-ray dose rates, or fast-neutron dose rates were measured is given in Table 2.

Table 2. Shielding Configurations Tested Behind ORR Beam Hole HB-2

No.	Configuration	Type of Measurement				
		Foil Spectral Measurement	Transmitted Fast-Neutron Dose Rate	Scattered Fast-Neutron Dose Rate <sup>a</sup>	Transmitted Gamma-Ray Dose Rate	Scattered Gamma-Ray Dose Rate <sup>a</sup>
0	Coffin Empty					
1	24 in. Barytes Concrete					
2	17 in. Barytes Concrete					
2a	3/8 in. Plexibor; 17 in. Barytes Concrete					
3	11 in. Barytes Concrete					
4	6 in. Barytes Concrete					
5	2 in. Barytes Concrete					
6	16 in. Borated Polyethylene; 6 in. Pb					
7	9 in. Borated Polyethylene; 6 in. Pb					
8	3 in. Borated Polyethylene; 6 in. Pb					
9	2 in. Air Gap; 16 in. Borated Polyethylene; 4 in. Pb					
10	4 in. Air Gap; 16 in. Borated Polyethylene; 2 in. Pb					
11	16 in. Air Gap; 16 in. Borated Polyethylene					
12	5-5/8 in. Air Gap; 3/8 in. Plexibor; 16 in. Borated Polyethylene					
13	4 in. Air Gap; 10 in. Fe; 8 in. Borated Polyethylene					
14	3/8 in. Air Gap; 16 in. Borated Polyethylene; 6 in. Polyethylene; 2 in. Pb					
15	1-3/8 in. Air Gap; 1 in. Fe; 16 in. Borated Polyethylene; 6 in. Pb					
16	1 in. Air Gap; 3/8 in. Plexibor; 1 in. Fe; 16 in. Borated Polyethylene; 6 in. Pb					
17	3/8 in. Air Gap; 2 in. Fe; 16 in. Borated Polyethylene; 6 in. Pb					
18	3/8 in. Plexibor; 2 in. Fe; 16 in. Borated Polyethylene; 6 in. Pb					
19	3/8 in. Air Gap; 4 in. Fe; 14 in. Borated Polyethylene; 6 in. Pb					
20	3/8 in. Plexibor; 4 in. Fe; 14 in. Borated Polyethylene; 6 in. Pb					
21	16 in. Polyethylene; 6 in. Pb					
22	3/8 in. Plexibor; 16 in. Polyethylene; 6 in. Pb					
23	3/8 in. Plexibor; 24 in. Barytes Concrete					

Table 2 (Continued)

No.	Configuration	Type of Measurement				
		Foil Spectral Measurement	Transmitted Fast-Neutron Dose Rate	Scattered Fast-Neutron Dose Rate <sup>a</sup>	Transmitted Gamma-Ray Dose Rate	Scattered Gamma-Ray Dose Rate <sup>a</sup>
24	3/4 in. Air Gap; 3/8 in. Plexibor; 2 in. Pb; 21 in. Barytes Concrete					
25	3/4 in. Air Gap; 3/8 in. Plexibor; 21 in. Barytes Concrete; 2 in. Pb					
26	6-3/4 in. Air Gap; 6 in. Pb; 11 in. Barytes Concrete					
27	6-3/4 in. Air Gap; 6 in. Fe; 8 in. Borated Polyethylene					
28	24 in. Barytes Concrete; 2 in. Pb					
29	20 in. Barytes Concrete; 6 in. Pb					
30	10 in. Air Gap; 10 in. Barytes Concrete; 6 in. Pb					
31	20 in. Air Gap; 6 in. Pb					
32	14 in. Borated Polyethylene; 10 in. Fe					
33	10 in. Fe; 14 in. Borated Polyethylene					
34	4 in. Borated Polyethylene; 1 in. Fe; 1 in. Borated Polyethylene; Alt. for 20 in.					
35	16 in. Barytes Concrete; 6 in. Pb					
36	17 in. Air Gap; 3 in. Borated Polyethylene; 6 in. Pb					
37	7 in. Air Gap; 17 in. Barytes Concrete					
38	7 in. Air Gap; 10 in. Fe; 8 in. Borated Polyethylene					

a. Scattered Dose was measured only in front duct, except for configuration 0, with which scattered dose was also measured in the rear duct.

EXPERIMENTAL RESULTSNeutron Spectra

Results of neutron energy spectrum measurements for the unattenuated beam (Conf. 0) and behind various thicknesses of barytes concrete, Figs. 3 and 4, plus measurements behind a borated polyethylene--lead combination and a Plexibor--concrete configuration, are given in Table 3. The spectrum above thermal energy is presented as the number of neutrons with energy greater than the reaction threshold energy of the foils. A 2-in. thickness of concrete placed in the beam caused a sharp reduction in the relative thermal and low-energy neutron intensity, as evident in Fig. 4, but thicknesses beyond 6 in. made little change in the spectral shape. The high-energy neutron region was attenuated with a relaxation length of about 8 cm.

Fast-Neutron Dose Rates

The fast-neutron dose rate behind a variety of configurations is presented in Table 4. Some interesting comparisons may be noted. From the data behind configurations 32 and 33, it is seen that placing 10 in. of iron in front of 14 in. of borated polyethylene reduced the dose rate a factor of about three compared to the dose with the same components reversed. From configuration 34, it is seen that altering the iron and borated polyethylene slabs was not as effective as using all of the iron in front. Likewise, 6 in. of lead preceding 11 in. of concrete (Conf. 26) showed a factor of about 6 greater attenuation than when the configuration was reversed. Six in. of lead in front of 11 in. of concrete produced about the same attenuation as 16 in.

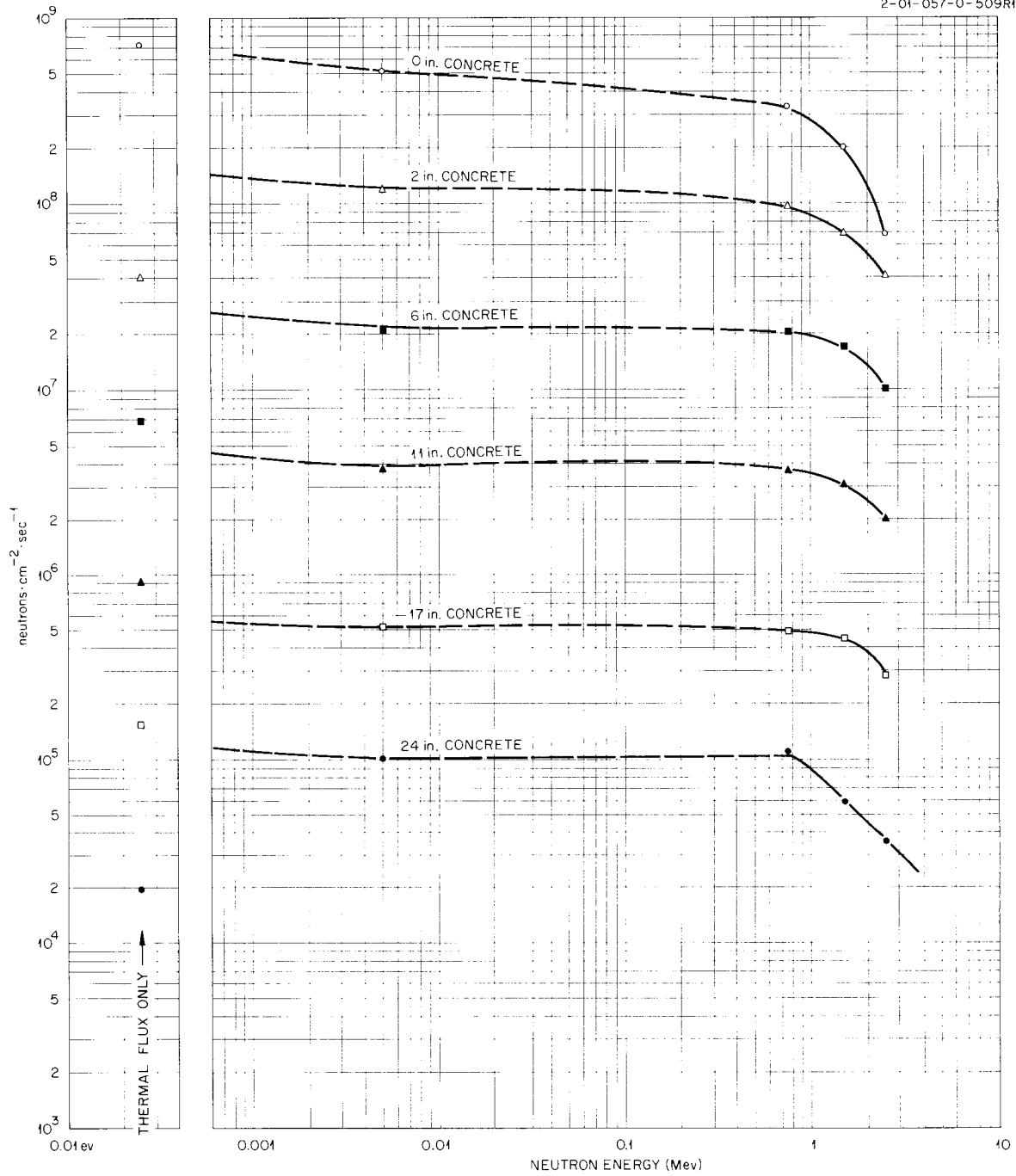


Fig. 3. Integrated Neutron Flux Above Energy E, Plotted as a Function of E. Flux measured by threshold foil detectors.

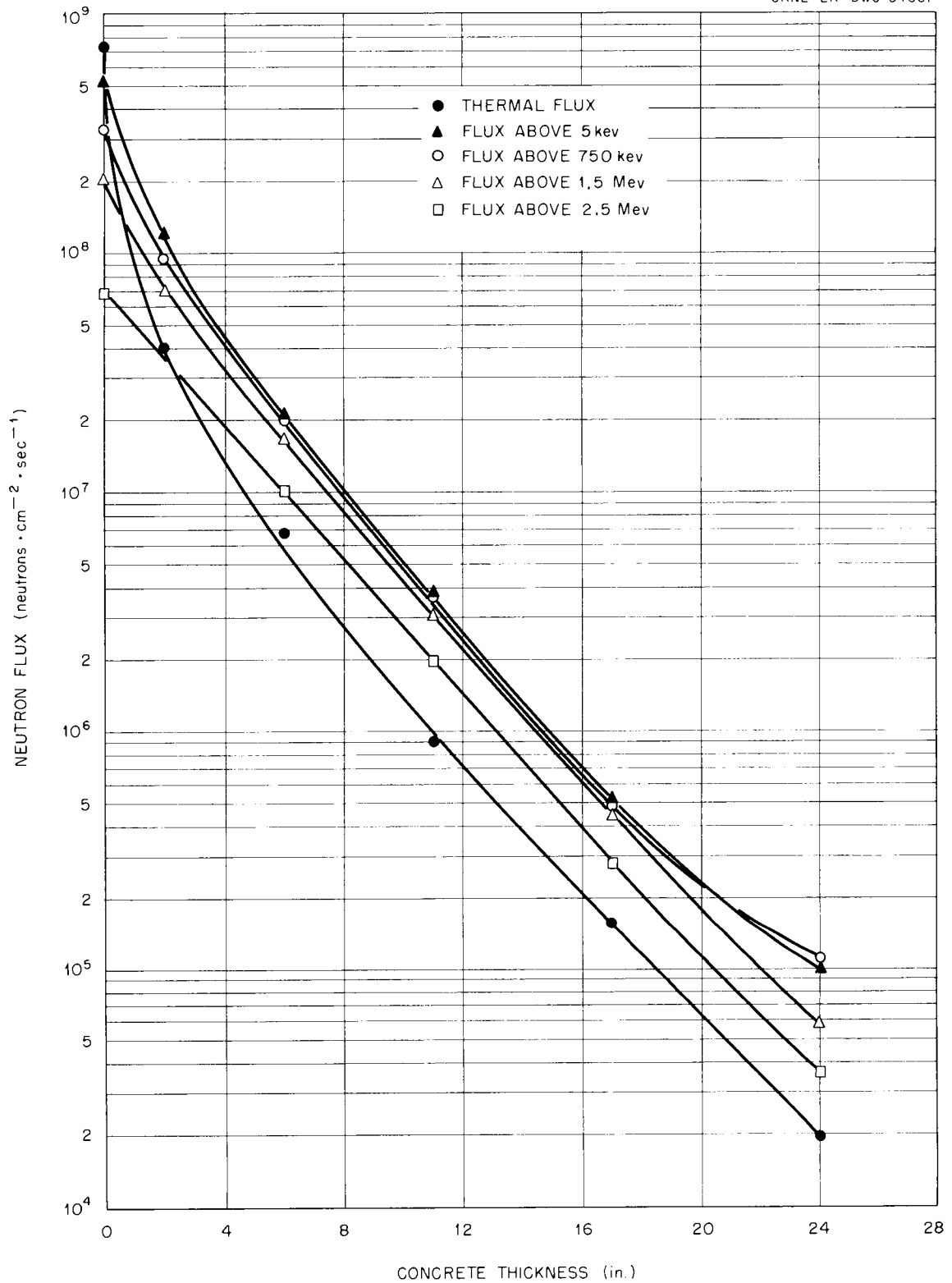


Fig. 4. Neutron Flux as a Function of Concrete Thickness.

Table 3. Neutron Energy Spectral Data Behind Various Shielding Configurations

Conf. No.	Flux (neutrons.cm <sup>-1</sup> .sec <sup>-1</sup> )						Dose (ergs.g <sup>-1</sup> .hr <sup>-1</sup> )		
	Bare Au	Cd-Covered Au	Thermal Flux	Pu	Np	U	X	Experiment	Normalized <sup>b</sup>
0	8.64 x 10 <sup>8</sup>	1.41 x 10 <sup>8</sup>	7.23 x 10 <sup>8</sup>	5.24 x 10 <sup>8</sup>	3.27 x 10 <sup>8</sup>	1.99 x 10 <sup>8</sup>	6.74 x 10 <sup>7</sup>	4.21 x 10 <sup>5</sup>	4.08 x 10 <sup>5</sup>
1	3.01 x 10 <sup>4</sup>	1.04 x 10 <sup>4</sup>	1.97 x 10 <sup>4</sup>	1.01 x 10 <sup>5</sup>	1.10 x 10 <sup>5</sup>	5.88 x 10 <sup>4</sup>	3.62 x 10 <sup>4</sup>	1.14 x 10 <sup>2</sup>	1.10 x 10 <sup>2</sup>
2	2.29 x 10 <sup>5</sup>	7.26 x 10 <sup>4</sup>	1.56 x 10 <sup>5</sup>	5.15 x 10 <sup>5</sup>	4.84 x 10 <sup>5</sup>	4.47 x 10 <sup>5</sup>	2.83 x 10 <sup>5</sup>	5.99 x 10 <sup>2</sup>	5.80 x 10 <sup>2</sup>
3	1.31 x 10 <sup>6</sup>	4.00 x 10 <sup>5</sup>	9.10 x 10 <sup>5</sup>	3.75 x 10 <sup>6</sup>	3.64 x 10 <sup>6</sup>	3.07 x 10 <sup>6</sup>	1.98 x 10 <sup>6</sup>	4.36 x 10 <sup>3</sup>	4.22 x 10 <sup>3</sup>
4	9.45 x 10 <sup>6</sup>	2.64 x 10 <sup>6</sup>	6.81 x 10 <sup>6</sup>	2.09 x 10 <sup>7</sup>	2.01 x 10 <sup>7</sup>	1.69 x 10 <sup>7</sup>	1.01 x 10 <sup>7</sup>	2.39 x 10 <sup>4</sup>	2.31 x 10 <sup>4</sup>
5	6.11 x 10 <sup>7</sup>	2.10 x 10 <sup>7</sup>	4.01 x 10 <sup>7</sup>	1.20 x 10 <sup>8</sup>	9.63 x 10 <sup>7</sup>	6.93 x 10 <sup>7</sup>	4.11 x 10 <sup>7</sup>	1.175 x 10 <sup>5</sup>	1.13 x 10 <sup>5</sup>
5 <sup>a</sup>	1.37 x 10 <sup>9</sup>	2.33 x 10 <sup>8</sup>	1.16 x 10 <sup>9</sup>	5.25 x 10 <sup>8</sup>	3.56 x 10 <sup>8</sup>	2.14 x 10 <sup>8</sup>	1.23 x 10 <sup>8</sup>	4.58 x 10 <sup>5</sup>	4.43 x 10 <sup>5</sup>
23	3.25 x 10 <sup>4</sup>	1.14 x 10 <sup>4</sup>	2.14 x 10 <sup>4</sup>	6.61 x 10 <sup>4</sup>	7.21 x 10 <sup>4</sup>	6.19 x 10 <sup>4</sup>	4.01 x 10 <sup>4</sup>	8.38 x 10 <sup>1</sup>	8.11 x 10 <sup>1</sup>
8	6.56 x 10 <sup>5</sup>	3.28 x 10 <sup>5</sup>	3.28 x 10 <sup>5</sup>	3.74 x 10 <sup>6</sup>	3.28 x 10 <sup>6</sup>	2.27 x 10 <sup>6</sup>	1.72 x 10 <sup>6</sup>	3.93 x 10 <sup>3</sup>	3.80 x 10 <sup>3</sup>

a. Scattered flux: foils exposed in Duct No. 1, 2 in. back, in the beam center line.

b. Normalization is discussed in text.

Table 4. Fast-Neutron Dose Rate Behind Various Shielding Configurations

Conf. No.	Dose Rate <sup>a</sup> (ergs·g <sup>-1</sup> ·hr <sup>-1</sup> )	Conf. No.	(ergs·g <sup>-1</sup> ·hr <sup>-1</sup> )	Notes
0	4.08 x 10 <sup>5</sup>	25	5.80 x 10 <sup>1</sup>	
1	1.10 x 10 <sup>2</sup>	26	1.26 x 10 <sup>2</sup>	
2	5.80 x 10 <sup>2</sup>	28	4.25 x 10 <sup>1</sup>	Rear beam shield removed
3	4.22 x 10 <sup>3</sup>	29	3.67 x 10 <sup>1</sup>	
4	2.31 x 10 <sup>4</sup>		8.79 x 10 <sup>-1</sup>	1/2- x 1/2-in. beam hole
5	1.13 x 10 <sup>5</sup>	30	5.06 x 10 <sup>2</sup>	
6	1.41 x 10 <sup>1</sup>		2.32 x 10 <sup>1</sup>	1/2- x 1/2-in. beam hole
7	7.37 x 10 <sup>1</sup>	31	5.16 x 10 <sup>2</sup>	1/2- x 1/2-in. beam hole
8 <sup>b</sup>	1.12 x 10 <sup>3</sup>	32	2.82 x 10 <sup>0</sup>	
13	9.42 x 10 <sup>0</sup>		6.84 x 10 <sup>-2</sup>	1/2- x 1/2-in. beam hole
15	9.94 x 10 <sup>0</sup>	33	8.61 x 10 <sup>-1</sup>	
16	8.53 x 10 <sup>0</sup>		2.03 x 10 <sup>-2</sup>	1/2- x 1/2-in. beam hole
17	5.31 x 10 <sup>0</sup>	34	1.16 x 10 <sup>0</sup>	
18	4.73 x 10 <sup>0</sup>		3.26 x 10 <sup>-2</sup>	1/2- x 1/2-in. beam hole
19	3.20 x 10 <sup>0</sup>	35	1.14 x 10 <sup>2</sup>	
20	3.04 x 10 <sup>0</sup>		3.50 x 10 <sup>0</sup>	1/2- x 1/2-in. beam hole
21	2.01 x 10 <sup>0</sup>	36	1.25 x 10 <sup>3</sup>	
22	1.97 x 10 <sup>1</sup>	38	1.08 x 10 <sup>1</sup>	
24	5.26 x 10 <sup>1</sup>			

a. Data was taken with 3- x 3-in. beam hole unless otherwise noted.

b. This measurement is questioned.

of concrete in front of 6 in. of lead. However, 2 in. of lead before 21 in. of concrete was only about 10% more effective than this shield with its layers reversed.

The data from configurations 0, 1, 2, 3, 4, and 5 have been plotted in Fig. 5 to show the fast-neutron dose rate as a function of concrete thickness. In these measurements the thickness was varied by removing slabs from the front, or beam side, of the shield, thus keeping the last slab in a fixed position with respect to the foils. The straight-line portion of the curve indicates a relaxation length in barytes concrete of  $\sim 7.5$  cm. Data for very thick and very thin slabs lie above the straight line due to scattering in the permanent shield surrounding the foils.

In conjunction with the fast-neutron dose rate measurements behind various configurations, an attempt was made to measure the scattering from the samples up the front duct. Unfortunately the measured dose rate includes a contribution from neutrons penetrating the duct wall after scattering from sources other than directly below the duct opening, and, since the magnitude of this effect could not be estimated, the data presented carries this error. In addition, when the shield sample consisted of iron, lead, or a combination of these elements, the configurations were backed by polyethylene and concrete in order to encompass the same depth as the concrete and polyethylene shields, and a mixture of scattering characteristics resulted. Nevertheless, some general conclusions may be drawn from the measurements in the front duct.

As was noted above, in obtaining the data from configurations 1 through 5, concrete slabs were removed from the front or beam side of

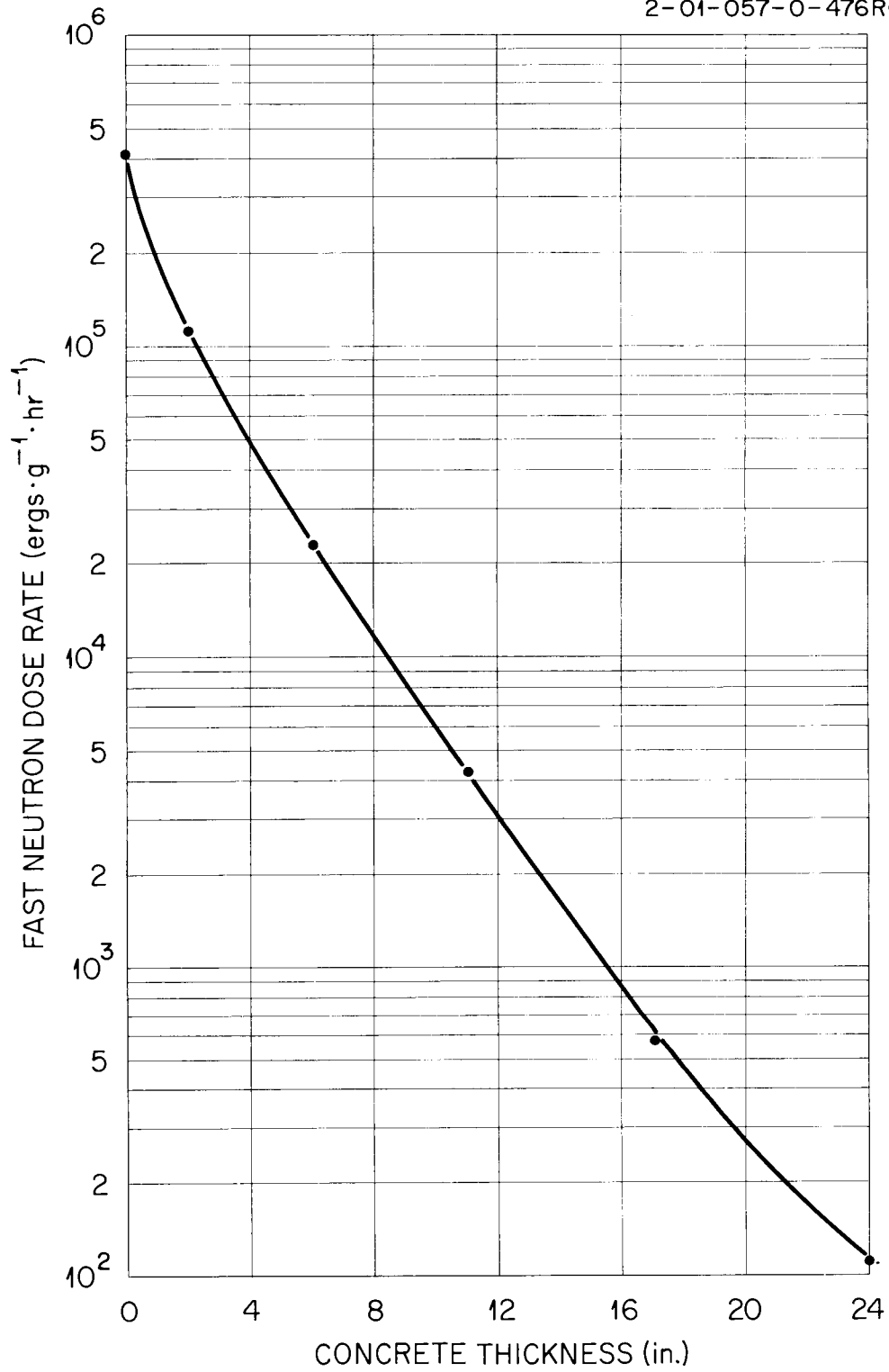
UNCLASSIFIED  
2-01-057-0-476R1

Fig. 5. Fast-Neutron Dose from ORR HB-2 as a Function of Thickness of Barytes Concrete.

the shield sample. This resulted in the front face of the sample being successively at the front edge of the coffin, the front edge of the duct, the back edge of the duct, and 5 in. beyond the back edge of the duct. The scattered fast-neutron dose rate in the front duct, plotted as a function of the position of the face of the concrete shield configuration, is shown in Fig. 6. The dose rate was a maximum when the shield face was at the front edge of the duct. Figure 7 summarizes all measurements of this type performed, and permits some gross inferences. For instance, it is apparent that lead scattered more than iron; both more than concrete. This agrees with the attenuation results previously discussed, in which either iron or lead preceding concrete reduced the intensity behind the shield. Scattering from polyethylene was a factor of about 5 less than from concrete.

During the tests of concrete shield configurations in the direct beam, measurements of the scattered dose in the front duct were made as a function of the thickness of concrete absorbers placed in the lower portion of the duct.\* The slopes of the curves obtained are about the same, and show a surprisingly long relaxation length of  $\sim 12$  cm. The thin absorber--thick shield data, however, shows a slight deviation above the straight line, suggesting a low-energy component. This data, along with data from other combinations of absorbers and shields, is given in Table 5. The attenuation qualities of concrete and lead may be compared, showing a difference in relaxation lengths of about a factor of 2, lead giving 6 cm vs. 11.7 for concrete.

---

\* It will be recalled that materials placed in the front duct to attenuate scattered radiation are arbitrarily called "absorbers," those in the direct beam are "shields" or "shielding configurations."

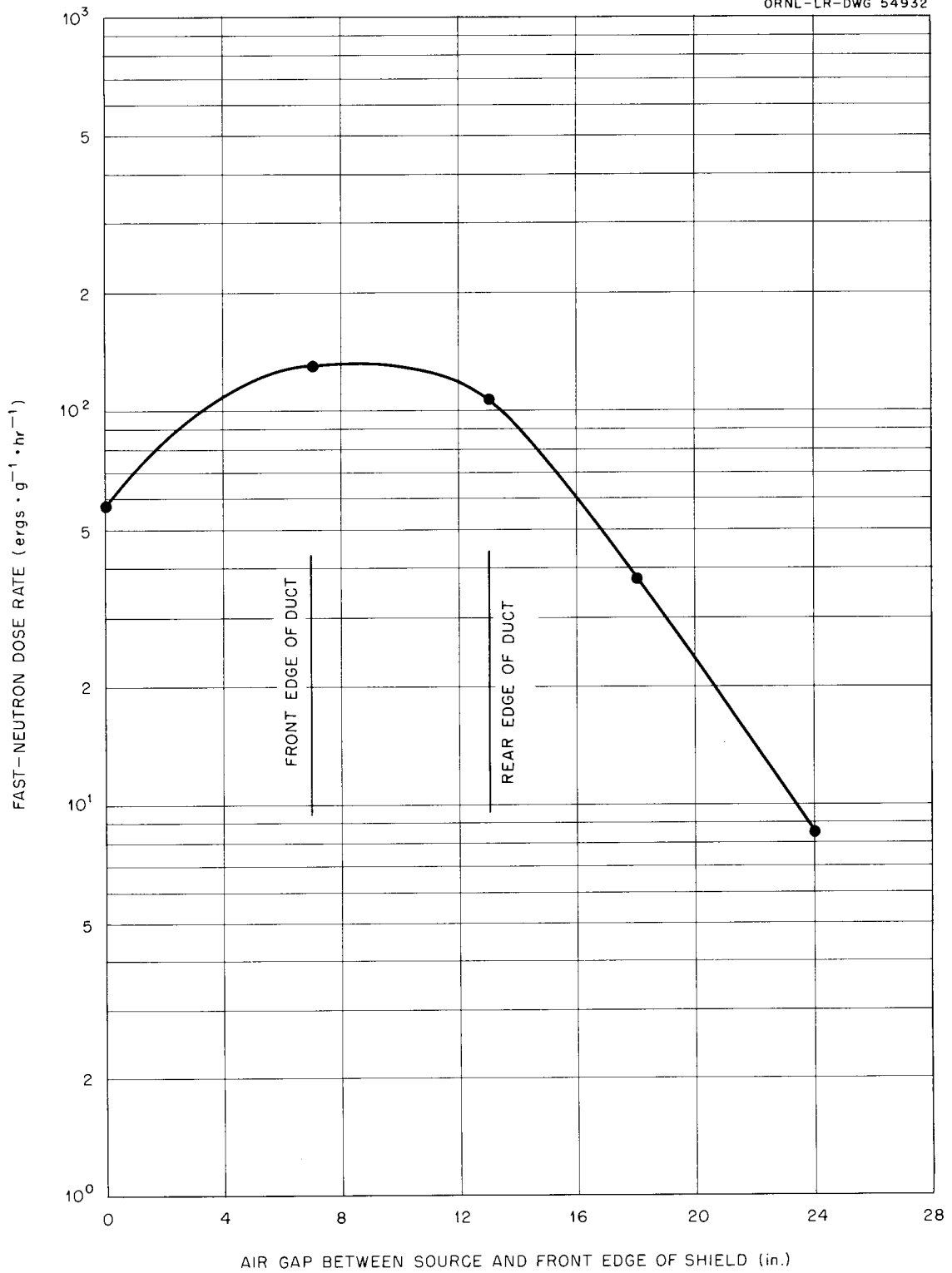
UNCLASSIFIED  
ORNL-LR-DWG 54932

Fig. 6. Scattered Fast-Neutron Dose Rate in Front Duct as a Function of Position of Face of Barytes Concrete Shield.

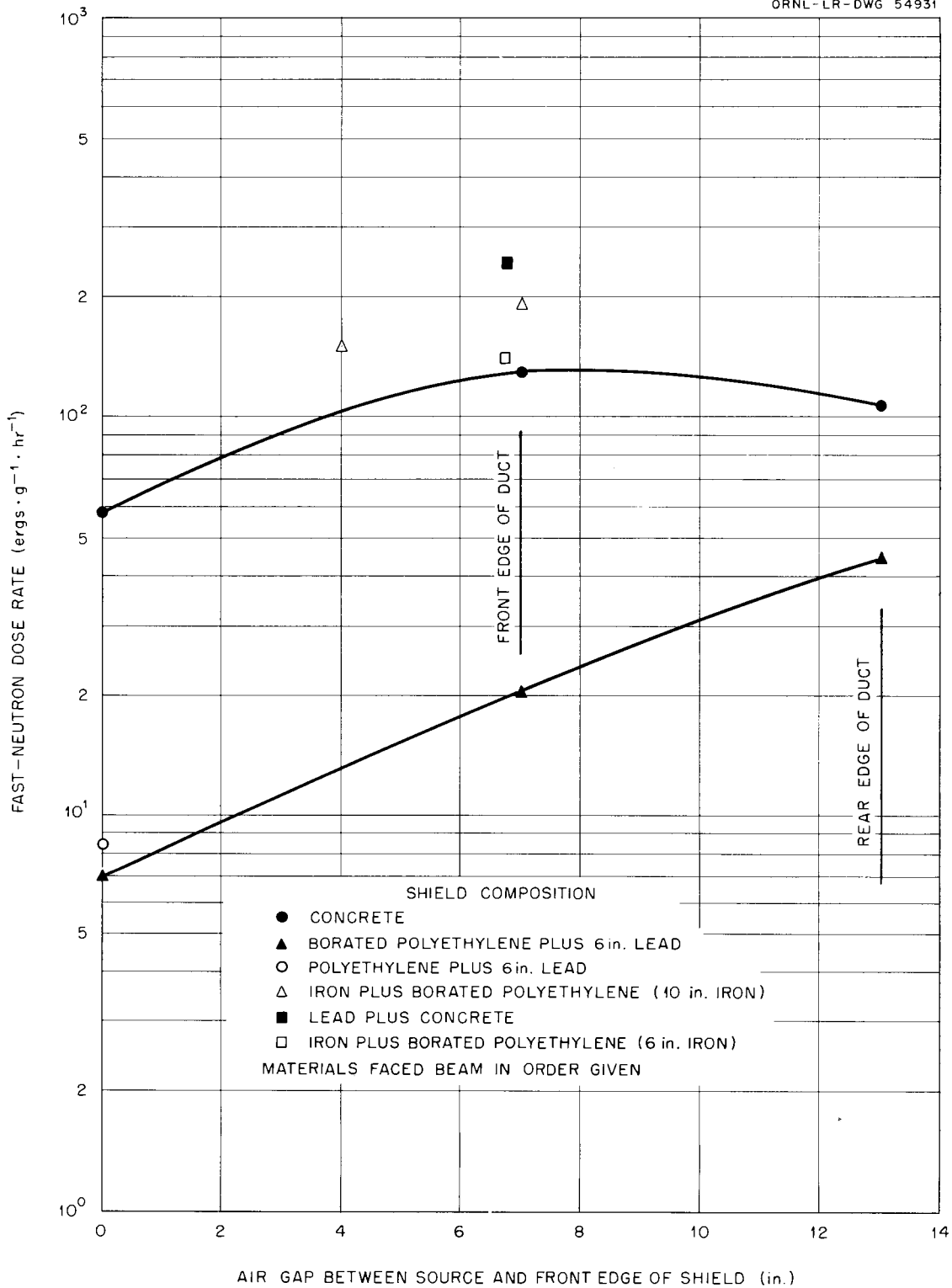


Fig. 7. Scattered Fast-Neutron Dose Rate in the Front Duct as a Function of Shield Position, for Various Shields Placed in the Direct Beam.

Table 5. Fast-Neutron Dose Rate in  $\text{ergs}\cdot\text{g}^{-1}\cdot\text{hr}^{-1}$ , in Front Duct  
as a Function of Absorber Thickness for Various Absorbers  
and Shield Configurations

Conf. No.	Absorber Thickness (in.)						
	0	1/2	1-1/2	2-1/2	3-1/2	4-1/2	5-1/2
Concrete Absorber							
	$\times 10^1$	$\times 10^1$	$\times 10^1$	$\times 10^1$	$\times 10^1$	$\times 10^1$	$\times 10^1$
0	0.866	0.780	0.629	0.499	0.411		0.279
1	5.77	4.66	3.68	2.91	2.33	1.89	1.56
2	12.9	10.0	7.52	5.84	4.63	3.71	2.98
3	10.7	8.85	6.85	5.15	4.12	3.27	2.68
4	3.76	3.33	2.65	2.16	1.77	1.42	1.17
6	0.696	0.538	0.454	0.356	0.297	0.244	0.206
7	2.05	1.65	1.32	1.02	0.848	0.672	0.565
13	15.4	11.7	8.82	6.23	4.84	3.64	2.92
21 <sup>a</sup>	0.839	0.610	0.492	0.408	0.332	0.285	
26	24.1	20.5	14.9	10.3	7.93	5.84	4.63
27	13.8	11.4	7.86	5.63	3.95		2.05
Lead Absorber							
	$\times 10^1$	$\times 10^1$	$\times 10^1$	$\times 10^1$			
1 <sup>b</sup>	5.66	3.25	2.56	2.14			
Polyethylene Absorber							
	$\times 10^0$	$\times 10^0$	$\times 10^0$	$\times 10^0$	$\times 10^0$	$\times 10^0$	$\times 10^0$
6	6.96	4.81	3.58	2.63	2.07	1.58	
21	8.36	7.02	4.80	3.40	2.46	1.79	1.35
Borated Polyethylene Absorber							
	$\times 10^1$	$\times 10^1$	$\times 10^1$	$\times 10^1$	$\times 10^1$	$\times 10^1$	$\times 10^1$
6	0.633	0.528	0.354	0.248	0.181	0.132	
7	2.05	1.61	1.02	6.75	4.63	3.25	2.29
8	4.53	3.36	1.99	1.28	8.78	5.92	4.11
13	16.0	10.8	5.57	3.07	1.81		0.972
21	0.842	0.669	0.459	0.321	0.221	0.158	0.113
26	25.0	18.7	10.8	6.44	3.93	2.40	1.57
27	13.8	9.14	4.67	2.61	1.51	1.02	0.676
38	19.0	13.9	7.49	4.18	2.19	1.53	0.983

a. Values shown were measured at 0, 1, 2, 3, 4, and 5 in.

b. Values shown were measured at 0, 1, 1-1/2, and 2 in.

The scattered fast-neutron dose rate in the front duct with no absorber present is given in Table 6 for various configurations as a function of detector position within the duct. The "Rear Duct" data essentially gives a measure of the scattering taking place within the personnel shield.

Figure 8 compares the attenuations of the scattered fast-neutron dose in the front duct by concrete, polyethylene, and borated polyethylene when the shielding sample in the coffin was polyethylene followed by lead. For equal thicknesses, polyethylene was a much better attenuator than concrete. The slight improvement demonstrated by the borated polyethylene over the pure polyethylene would become almost negligible if the results were corrected for minor differences in thickness between the disks. The nominally 1-in.-thick polyethylene disks were more nearly  $31/32$  in. thick, while the borated disks were slightly thicker than 1 in. This correction has not been made to any of the data.

Figure 9 shows the scattered dose rate behind various thicknesses of concrete absorber for several other shielding configurations in the coffin. Comparison is hampered by the fact, previously noted, that the concrete and lead are backed by concrete, while the iron and polyethylene are followed by polyethylene. As was shown in Table 5, the scattering up the duct when concrete is placed at its rear edge is about twice that for polyethylene in the same location. Their respective contributions to the data of Fig. 9, however, are probably small. The slopes of the curves for air, polyethylene, and concrete are similar, giving relaxation lengths of  $\sim 11.5$  cm, while iron and lead give  $\sim 8$  cm. This admittedly incomplete data suggests that the neutron energy may be softer after scattering from iron or lead.

Table 6. Fast-Neutron Dose Rate in  $\text{ergs}\cdot\text{g}^{-1}\cdot\text{hr}^{-1}$  as a Function of Detector Position for Various Configurations

Conf. No.	Detector Position (cm) <sup>a</sup>				
	0	10	15	30	45
	Center Line of Rear Duct				
	$\times 10^1$	$\times 10^1$	$\times 10^1$	$\times 10^1$	$\times 10^1$
0	17.2	5.76	3.99	1.49	0.696
	Center Line of Front Duct				
	$\times 10^1$	$\times 10^1$	$\times 10^1$	$\times 10^1$	$\times 10^1$
1	5.58		2.72		0.951
2	12.4		7.13		3.00
3	10.7		5.41		1.73
4	3.76		1.55		0.428
7	2.07	1.34	1.10	0.669	0.443
8	4.44	2.69	2.07	1.16	0.680
13	15.2	10.3	8.43	5.11	3.33
22	0.796	0.478	0.372	0.211	0.127
26	24.1	17.2	14.8	9.68	6.53

a. Zero for these measurements was 52 cm below top of personnel shield, approximately 25 cm above top of sample coffin.

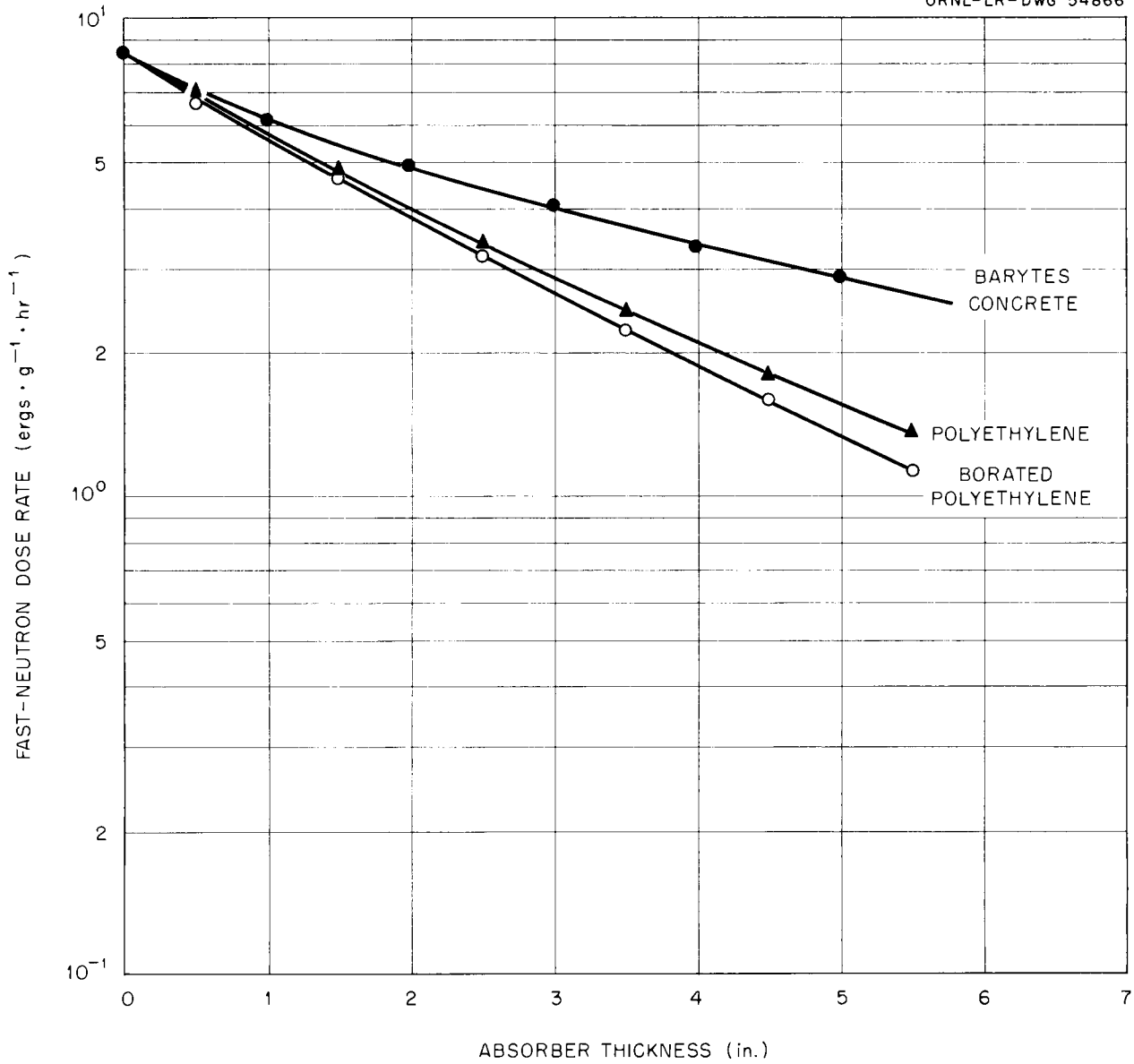
UNCLASSIFIED  
ORNL-LR-DWG 54866

Fig. 8. Fast-Neutron Dose Rate as a Function of Absorber Thickness for Various Absorbers Placed in Front Duct.

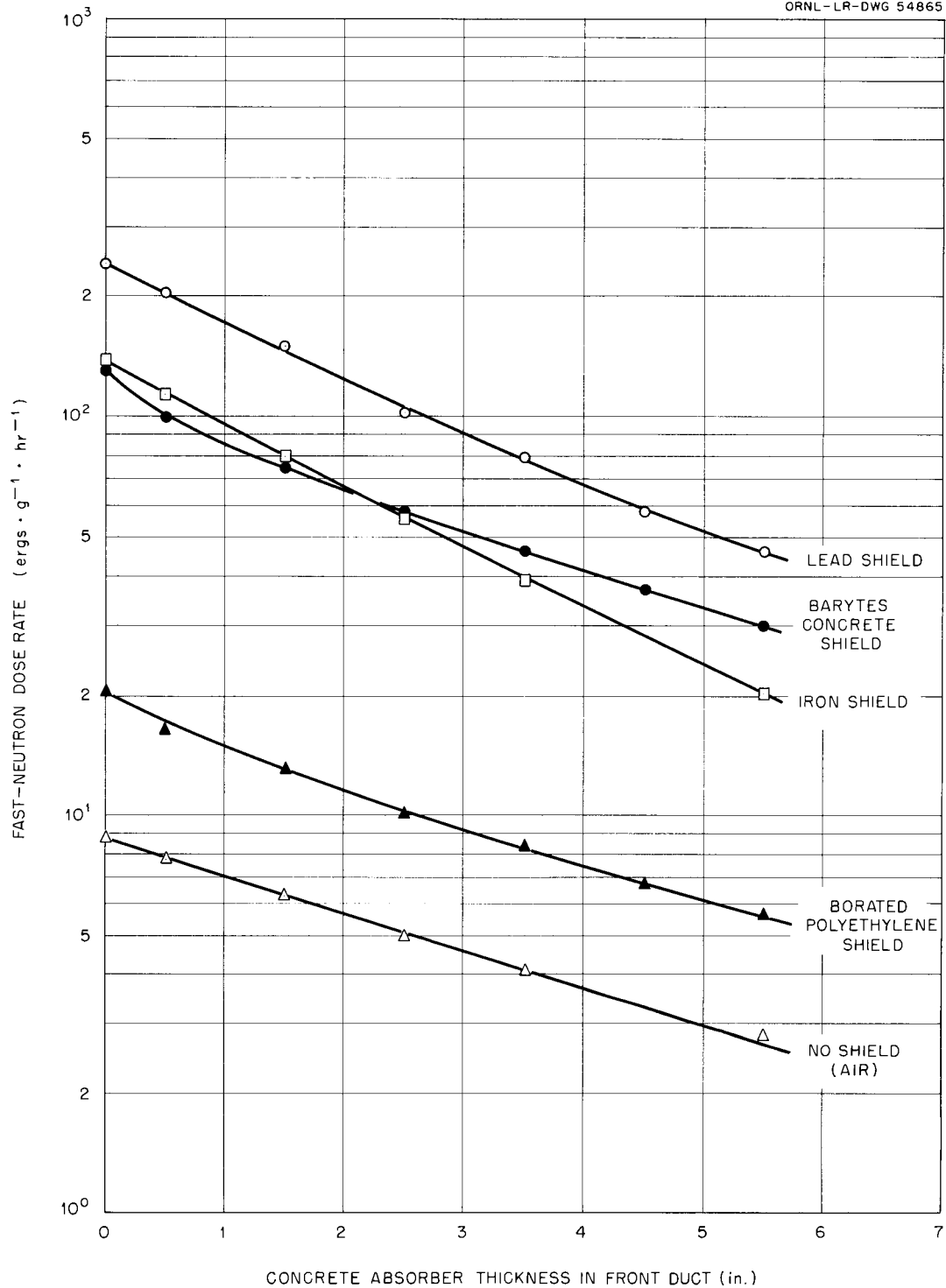


Fig. 9. Scattered Fast-Neutron Dose Rate Behind Barytes Concrete Absorbers in Front Duct, as a Function of Concrete Thickness, for Various Shields in the Direct Beam. A 7-in.-thick air gap is common to all shields.

### Gamma-Ray Dose Rates

Gamma-ray data was obtained in conjunction with the neutron data, and the same configurations, listed in Table 2, were used. No gamma-ray spectra were observed, because the gamma-ray flux was too high.

All gamma-ray dose rate data is presented in combined form in Table 7. The column headed "Transmitted Beam" represents the transmitted dose rate through the various configurations, while the other columns show scattered gamma-ray dose rates in the front duct for various conditions of absorber or detector position in the duct.

Dose rate measurements behind concrete shields are shown in Fig. 10 as a function of concrete thickness. The relaxation length,  $\sim 10$  cm, is about as expected. It should be noted that the addition of Plexibor to the front of the 24-in.-thick shield did not change the dose rate, and made only about a 10% difference when added to the 17-in.-thick shield.

The gamma-ray dose rate behind a combination of iron, 16 in. of borated polyethylene, and 6 in. of lead was measured as a function of iron thickness. The results indicate that 1 in. of iron reduced the dose rate about 50%, giving a relaxation length of 4.3 cm. Plexibor placed before the iron to reduce capture gamma rays gave only a 2 or 3% reduction in dose rate. When the lead was eliminated from the shield and the borated polyethylene thickness diminished to 8 in., the dose rate was reduced a factor of 10 by increasing the iron thickness from 6 to 10 in.

Another series of experiments consisted of gamma-ray dose measurements behind combinations of several materials in varying ratios. In this group were iron and borated polyethylene, borated polyethylene and

Table 7. Gamma-Ray Dose Rates Behind (or Scattered from) Various Shield Configurations

Conf. No.	Transmitted Beam	Gamma-Ray Dose Rate (ergs·g <sup>-1</sup> ·hr <sup>-1</sup> )								
		Scattered: Front Duct								
		0 in. Pb x 10 <sup>1</sup>	$\frac{1}{2}$ in. Pb x 10 <sup>1</sup>	1 in. Pb x 10 <sup>1</sup>	$1\frac{1}{2}$ in. Pb x 10 <sup>1</sup>	2 in. Pb x 10 <sup>1</sup>	3 in. Pb	0 cm Air	15 cm Air	30 cm Air
0	1.84 x 10 <sup>6</sup>	12.7	10.0	8.68	7.54	6.82				
1	3.76 x 10 <sup>3</sup>	23.4	13.0	9.49	6.84	5.47				
2	2.97 x 10 <sup>4</sup> (a)	82.0	45.5	30.7	22.0	16.5	x 10 <sup>2</sup>	x 10 <sup>2</sup>	x 10 <sup>2</sup>	
2A	1.77 x 10 <sup>4</sup>	38.6	20.6	14.4	10.7	7.93		1.92	1.14	
3	9.17 x 10 <sup>4</sup>	129	79.7	55.7	39.6	31.0	12.7	5.73	2.87	
4	3.18 x 10 <sup>5</sup>	75.1(c)	48.5	35.4	26.0	20.3	7.52	3.07	1.45	
5	9.96 x 10 <sup>5</sup> (d)									
6	2.34 x 10 <sup>2</sup>	32.9	4.63	2.41	1.78	1.31				
7	4.61 x 10 <sup>2</sup>	63.0	14.4	9.42	6.58	4.91				
8	1.25 x 10 <sup>3</sup>	89.2	45.0	32.5	23.4	18.0				
9	2.60 x 10 <sup>3</sup>									
10	2.93 x 10 <sup>4</sup>									
11	3.31 x 10 <sup>5</sup>									
12	3.11 x 10 <sup>5</sup>									
13	8.69 x 10 <sup>2</sup>	33.6	23.8	18.5	14.7	12.1				
14	2.00 x 10 <sup>4</sup>									
15	1.42 x 10 <sup>2</sup>									
16	1.38 x 10 <sup>2</sup>									
17	7.07 x 10 <sup>1</sup>									
18	6.85 x 10 <sup>1</sup>									
19	2.29 x 10 <sup>1</sup>									
20	2.21 x 10 <sup>1</sup>									

Table 7 (Continued)

Conf. No.	Gamma-Ray Dose Rate (ergs·g <sup>-1</sup> ·hr <sup>-1</sup> )									
	Transmitted Beam	Scattered: Front Duct								
		0 in. Pb x 10 <sup>1</sup>	$\frac{1}{2}$ in. Pb x 10 <sup>1</sup>	1 in. Pb x 10 <sup>1</sup>	$1\frac{1}{2}$ in. Pb x 10 <sup>1</sup>	2 in. Pb x 10 <sup>1</sup>	3 in. Pb	0 cm Air	15 cm Air	30 cm Air
26	4.21 x 10 <sup>2</sup>	78.5	63.3	53.6	45.8	39.8				
27	98.9 x 10 <sup>2</sup>	39.6	36.0	30.0	25.4	22.2				
28	4.22 x 10 <sup>2</sup>									
29	0.164 x 10 <sup>2</sup> (e)									
30	2.55 x 10 <sup>2</sup> (f)									
31	55.7 x 10 <sup>2</sup> (g)									
32	6.20 x 10 <sup>2</sup> (h)									
33	4.86 x 10 <sup>2</sup> (j)									
34	5.59 x 10 <sup>2</sup> (k)									
35	0.545 x 10 <sup>2</sup>									
36	17.2 x 10 <sup>2</sup>	48.2								
37	20.6 x 10 <sup>2</sup>									
38	9.74 x 10 <sup>2</sup>	48.7	37.7	31.6	26.9	24.0	18.9			

- a. This value is believed too high.  
b. Average of two values,  $2.93 \times 10^5$  and  $3.43 \times 10^5$ .  
c. Dose at Center Line of coffin,  $2.56 \times 10^6$ .  
d. Average of  $1.01 \times 10^6$  and  $9.91 \times 10^5$ .  
e. Measurement with 1/2-in. x 1/2-in. hole in shutter gave  $3.78 \times 10^0$ .  
f. Measurement with 1/2-in. x 1/2-in. hole in shutter gave  $1.64 \times 10^1$ .  
g. Measurement with 1/2-in. x 1/2-in. hole in shutter gave  $2.15 \times 10^2$ .  
h. Measurement with 1/2-in. x 1/2-in. hole in shutter gave  $3.39 \times 10^1$ .  
j. Measurement with 1/2-in. x 1/2-in. hole in shutter gave  $2.46 \times 10^1$ .  
k. Measurement with 1/2-in. x 1/2-in. hole in shutter gave  $3.27 \times 10^1$ .

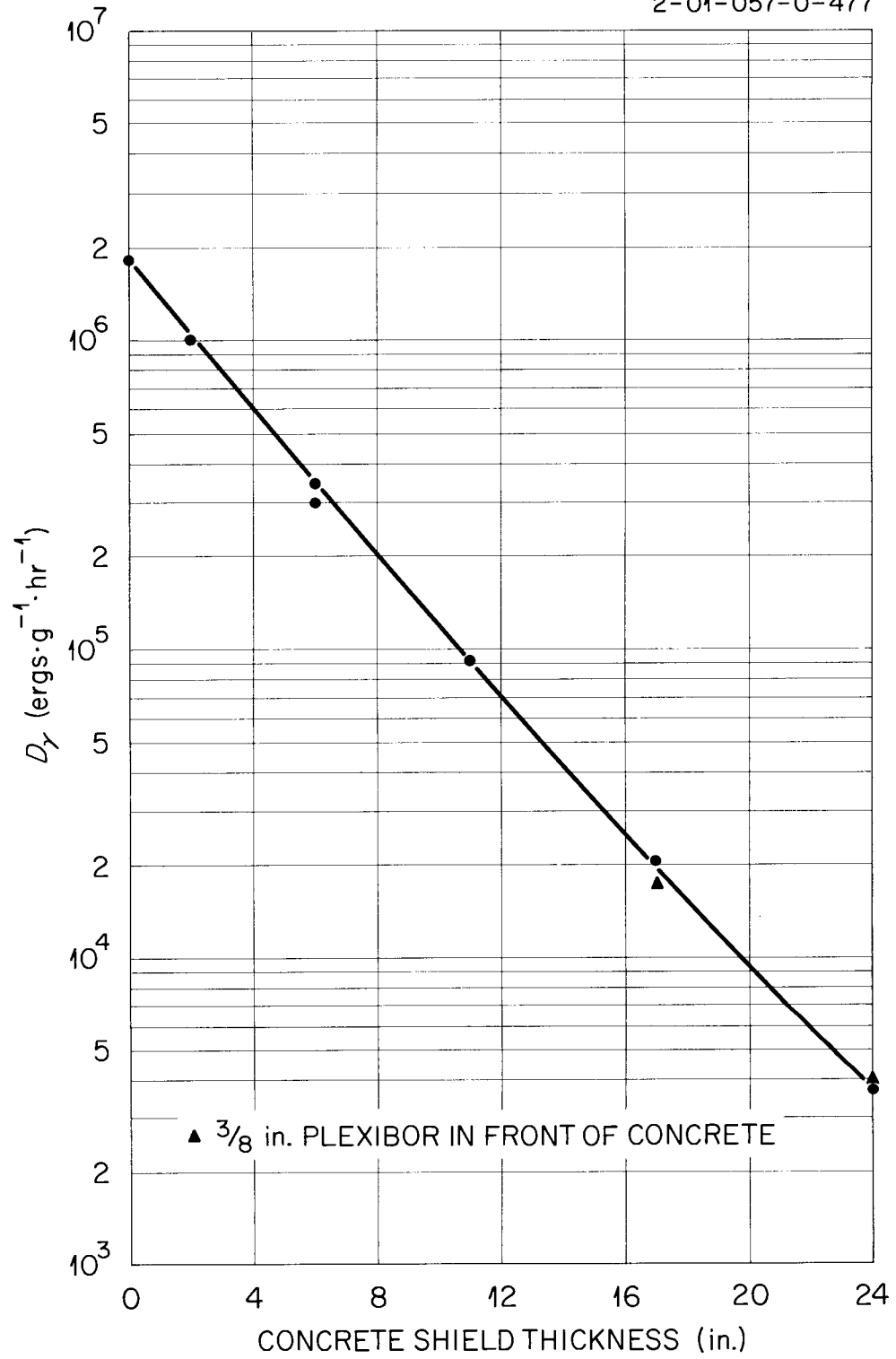
UNCLASSIFIED  
2-01-057-0-477

Fig. 10. Gamma-Ray Dose Rate from ORR HB-2 as a Function of Thickness of Barytes Concrete Shield.

lead, and concrete and lead. The results from borated polyethylene and lead, and concrete and lead, are shown in Fig. 11. As lead thickness was varied behind borated polyethylene, the dose rate behaved as expected, decreasing by a factor of 10 for each 2 in. of lead added. The sharp decrease in dose rate observed when borated polyethylene was placed in front of the lead results mainly from a decrease in lead captures plus a decrease in gamma rays from neutron scattering in lead. After the initial thickness of borated polyethylene is added, the slope is similar to that expected for borated polyethylene alone. When concrete was added in front of the lead, the initial drop in dose rate seemed to be much less than for borated polyethylene, but the exact shape is unknown since no data point was measured in this region. The relaxation length, however, is that expected of concrete.

The addition of  $3/8$  in. of Plexibor in front of 24 in. of concrete had negligible effect on either the dose rate behind the configuration or the component scattered up the front duct. With a configuration consisting of 16 in. of polyethylene followed by 6 in. of lead, the addition of  $3/8$  in. of Plexibor in front of the shield decreased the transmitted dose rate by  $\sim 7\%$ ; the scattered component by  $\sim 15\%$ . The substitution of borated polyethylene for the polyethylene and Plexibor reduced the scattered dose several per cent; the transmitted dose  $\sim 8\%$ .

A test of the preferred distribution of 10 in. of iron and 14 in. of borated polyethylene within a shield was made. The maximum dose rate behind the shield was observed when the borated polyethylene faced the beam; reversing the order so that the iron led reduced the dose rate

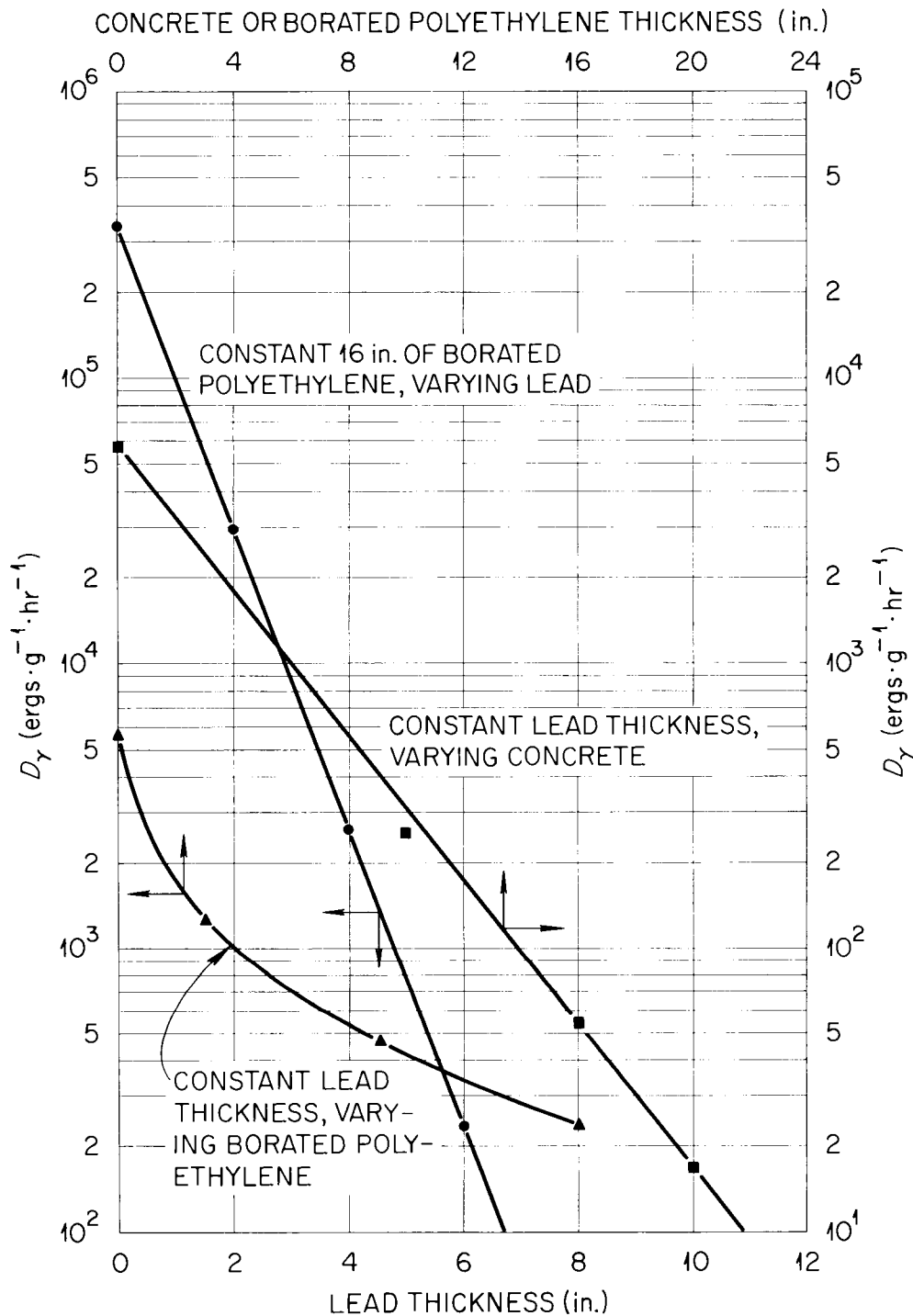


Fig. 11. Gamma-Ray Dose Rate from ORR HB-2 as a Function of Shield Thickness for Several Shield Configurations.

by 20%. A shield composed of alternate slabs of iron and borated polyethylene and preceded by 4 in. of borated polyethylene gave results about half way between the above.

Tests of lead--concrete combinations indicated that placing 2 in. of lead first before and then behind 21 in. of concrete gave dose rates within 7% identical when each shield was preceded by Plexibor. However, the dose rate behind a 6-in.-lead--11-in.-concrete shield was 65% greater than behind a 10-in.-concrete--6-in.-lead shield, with no Plexibor in either case. Alternating lead--borated polyethylene configurations were not examined.

The scattered gamma-ray dose rate in the front duct, plotted as a function of lead absorber thickness for various concrete shields in the direct beam, is shown in Fig. 12. The maximum scattered dose rate for gamma rays was observed when the front face of the concrete was at the rear of the duct. (For neutrons the dose rate was a maximum when the front face of the concrete was at the front edge of the duct.) Plexibor placed in front of the concrete reduced the scattered dose rate in the front duct by a factor of 2 for a 17-in.-thick concrete shield, but had no effect when used with a 24-in.-thick shield. It is of interest that the scattered dose rate measured for 6-in. and 17-in. concrete shields was about the same. A slight change in the slope of the curve of dose rate vs. lead absorber thickness, however, suggests a contribution from scattering through the personnel shield.

Scattering from a borated polyethylene shield was similar to that from concrete, the maximum dose rate being observed when the face of the shield was positioned at the rear of the front duct.

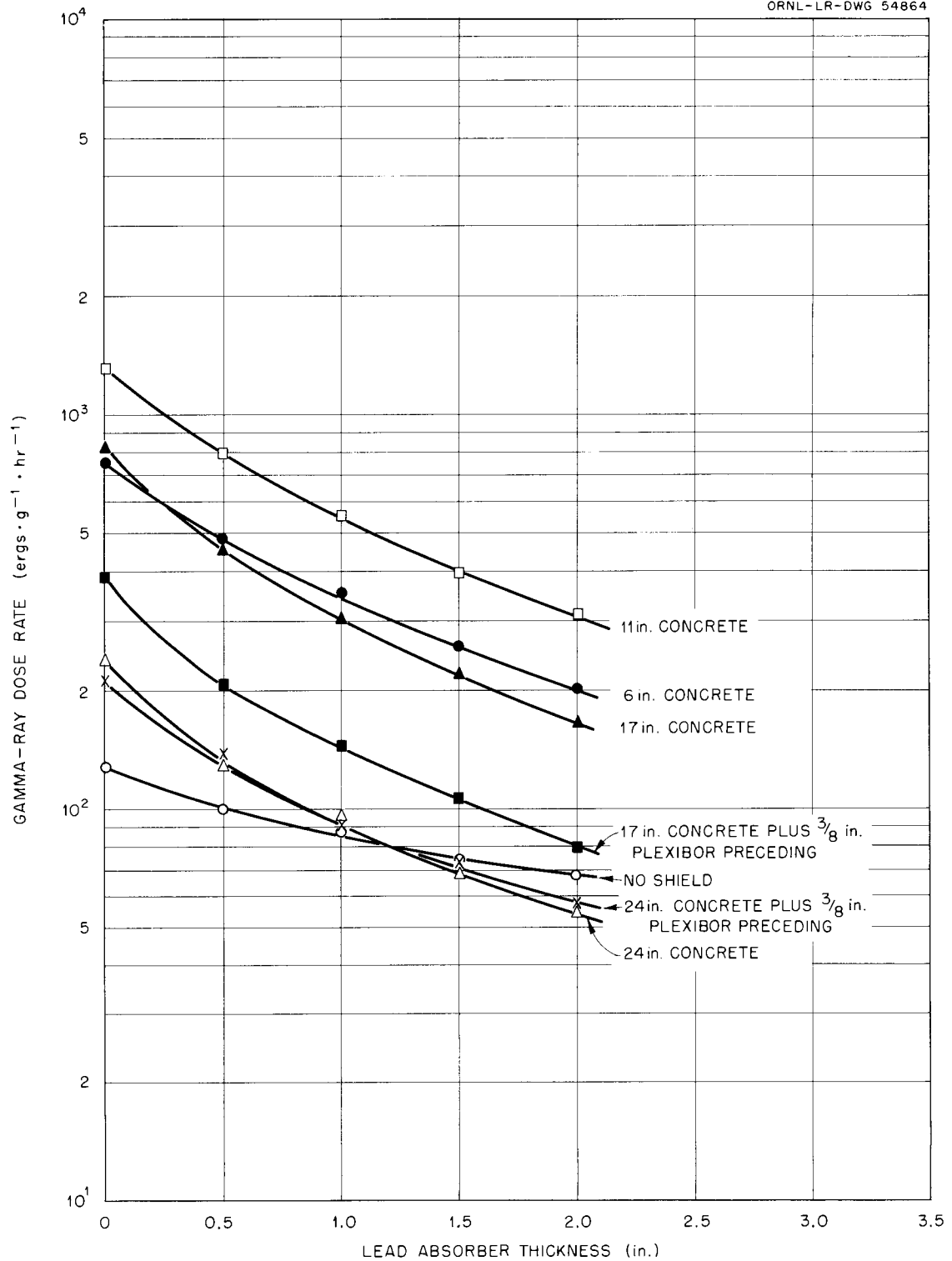
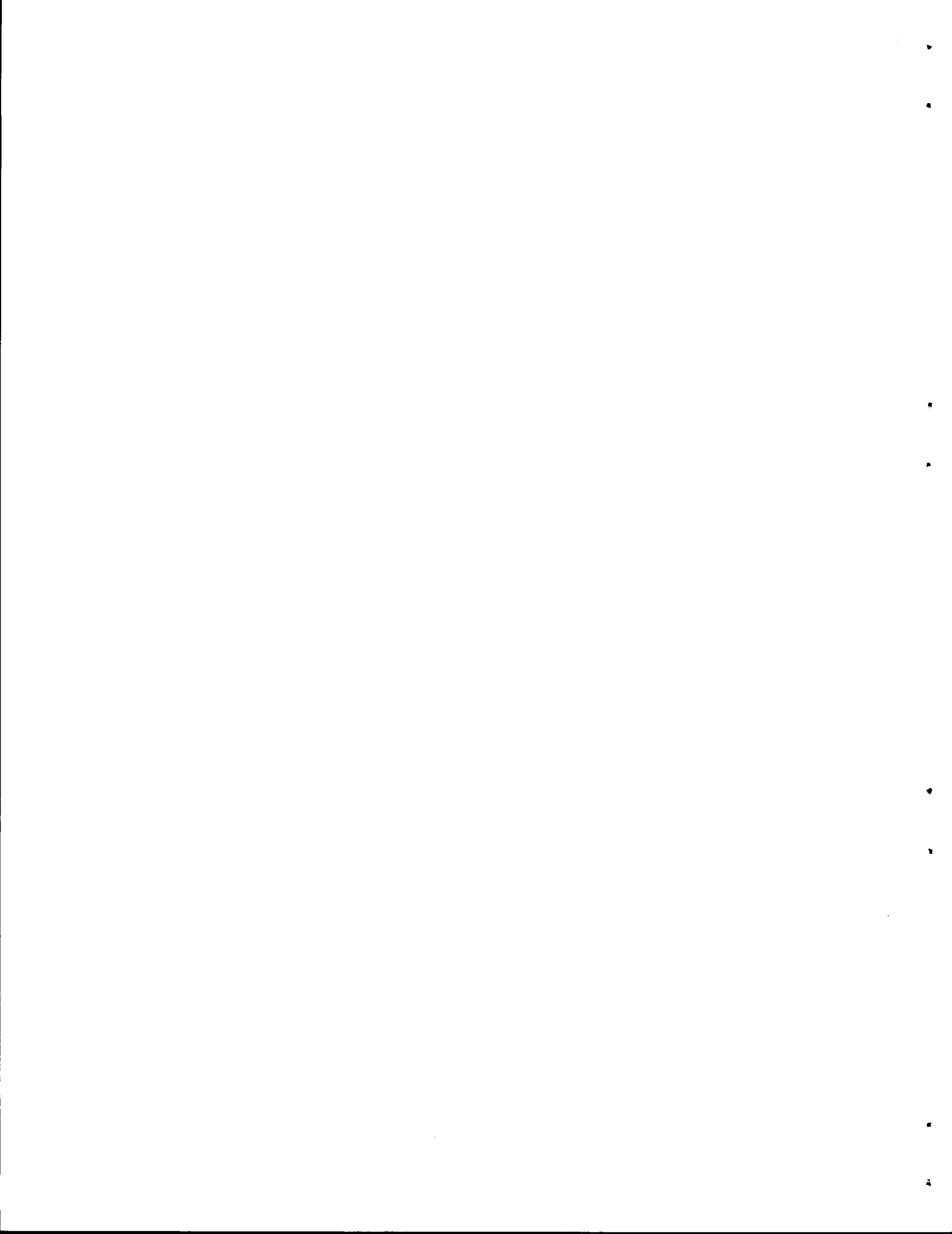


Fig. 12. Gamma-Ray Dose Rate as a Function of Thickness of Lead Absorber in Front Duct, for Various Shields Placed in the Direct Beam.



ORNL-3069  
 UC-34 Physics  
 TID-4500 (16th ed.)  
 December 15, 1960

## INTERNAL DISTRIBUTION

1.	C. E. Center	43.	W. H. Jordan
2.	Biology Library	44-48.	L. Jung
3.	Health Physics Library	49.	R. E. Maerker
4-6.	Central Research Library	50-59.	F. C. Maienschein
7.	Reactor Experimental Engineering Library	60-64.	J. M. Miller
8-31.	Laboratory Records Department	65-69.	F. J. Muckenthaler
32.	Laboratory Records, ORNL R.C.	70.	S. K. Penny
33.	E. P. Blizard	71.	J. A. Swartout
34-38.	T. V. Blosser	72.	D. K. Trubey
39.	V. R. Cain	73.	A. M. Weinberg
40.	R. A. Charpie	74.	P. F. Gast (consultant)
41.	J. A. Cox	75.	L. W. Nordheim (consultant)
42.	L. B. Holland	76.	R. F. Taschek (consultant)
		77.	T. J. Thompson (consultant)

## EXTERNAL DISTRIBUTION

78. Division of Research and Development, AEC, ORO  
 79-706. Given distribution as shown in TID-4500 (16th ed.) under Physics category (75 copies - OTS)